Bull. Min. Res. Exp. (2017) 155: 99-113

Bulletin of the Mineral Research and Exploration

http://bulletin.mta.gov.tr

WHOLE ROCK GEOCHEMISTRY AND TECTONIC SETTING OF JURASSIC AGED LISAR GRANITE, TALESH MOUNTAINS, NORTH IRAN

Roghieh BOZORG SEGHINSARA[a], Hossein SHEIKHI KARIZAKI[a], Mohssen MOAZZEN[b*], Mohsen POURKERMANI[a] and Afshin ASHJA ARDALAN[a]

[a]*Department of Geology, Azad Islamic University, North Tehran Branch, Tehran, Iran*
[b]*Department of Earth Sciences, University of Tabriz, 51664, Tabriz, Iran*
[b]*Tebriz Üniversitesi, Yer Bilimleri Bölümü, 51664, Tebriz, İran*

Research Article

Keywords:
A-type granite, Palaeotethys, Post-collision, Cimmerian, Talesh, North Iran.

ABSTRACT

The Late Jurassic aged Lisar granite in North Iran is in tectonic contact of the form of thrust and strike slip faults with Upper Cretaceous sandy limestone and is covered by Paleogene polygenetic conglomerate in the Talesh Mountain at the western continuation of the Alborz range. The rock samples of the granite are pink coloured and coarse-gained with K-feldspar, quartz, plagioclase, biotite and amphibole. The Lisar granite is more likely emplaced in an extensional environment indicated with numerous space filling silica-rich aplitic veins in the rocks. The granite samples are moderately altered and feldspars are changed to sericite and clay minerals and biotite is partially converted to chlorite. The Lisar granite has derived from a high K magma and is A-type in nature, belonging to A_2 subgroup. The rock samples of granite are characterized by distinct negative Eu anomaly and a decrease from LREE to HREE contents. The parental melts of the granite were generated from partial melting of a lower continental crustal source with possible contribution from the mantle materials. The Lisar granite represents Cimmerian post-collision magmatism in north Iran following closure of Palaeotethys Ocean and subsequent collision.

Received Date: 02.08.2016
Accepted Date: 19.04.2017

1. Introduction

Palaeomagnetic studies show that Iran was a part of Gondwana up to Early Carboniferous (Muttoni et al., 2009). It separated from Gondwana and moved northward from Early Permian to Upper Triassic, when it collided with Turan plate. The Alborz range is taken to represent Palaeotethys suture in north Iran (Figure 1) formed by collision of the Turan and the Iranian plates in Upper Triassic. The Jurassic aged Lisar granite is located in North Iran within the Talesh mountain range. The Talesh Mountain range is a continuation of the Alborz range towards the west. Rock units considered by different researchers to mark the Palaeotethys suture in North Iran are accretionary units of the Mashhad area (Alavi, 1991; Majidi, 1991; Mirnejad et al., 2013; Shafaii Moghdam et al., 2015), Gorgan schists (Ghavidel et al., 2007; Delaloy et al., 1981), metamorphic rocks of the Gasht and Masuleh area (Clark et al., 1975) and Shanderman eclogites (Zanchetta et al., 2009; Omrani et al., 2013). The Palaeotethys suture can be traced to the east to Afghanistan and China and towards the west into Turkey (Zhang et al., 2008). The Palaeotethys ocean closed 225 Ma ago which followed by uplifting of the Turan plate and emplacement of allochtonous nappes on the Iranian plate (Stampfli, 1993). Magmatic activities, especially granitoid magmatism, related to the Palaeotethys subduction are well documented along the suture in China. The magmatic arc at Yunnan area (southwestern Yunnan, China), with basaltic-andesitic to granodiorite composition has an age of 292- 282 Ma (Hennig et al., 2009). I-type and S-type granitoids of Hindu Kush in Afghanistan have ages of 210, 112 and 193 Ma, respectively (Debon et al., 1987). These granites with roughly Triassic age are traced westward into east of Iran, where the Binalud granites and granodiorites, dated 256 to 211 Ma (Majidi, 1978; Berberian and Berberian, 1981), are intruded into

* *Corresponding author: Mohssen MOAZZEN moazzen@tabrizu.ac.ir*
http://dx.doi.org/10.19111/bulletinofmre.336499

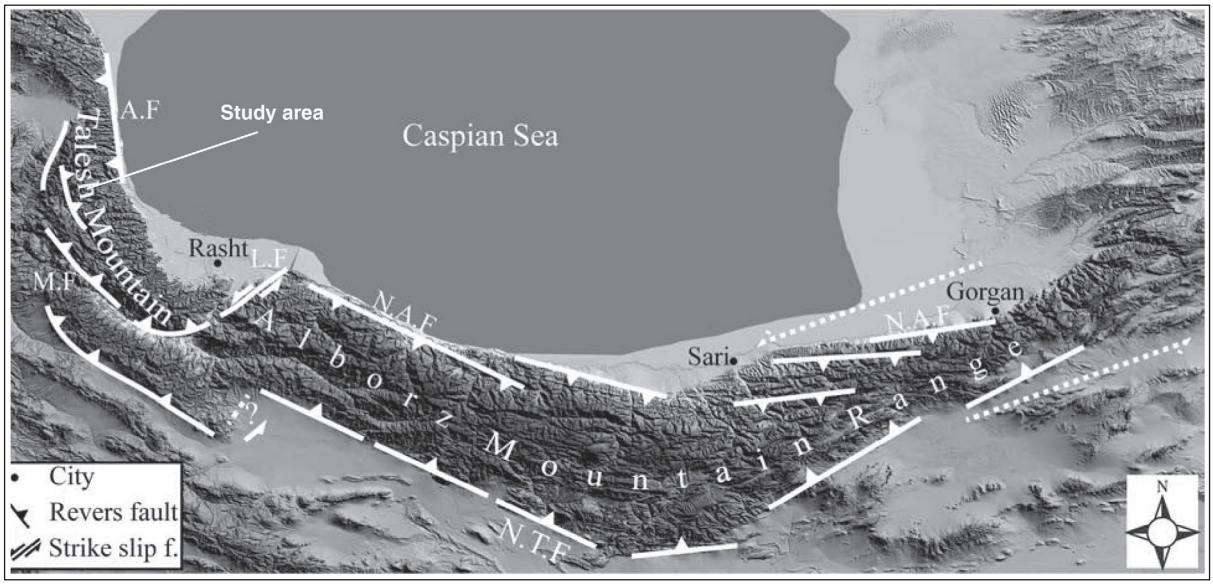

Figure 1- The location of the study area in Talesh Mountains at the west of Alborz range. AF: Astara Fault, MF: Masuleh Fault, LF: Lahijan Fault, NAF: North Alborz Fault, NTF: North Tehran Fault.

the Hercynian sediments. Boulin (1981) considered that they are a result of Palaeotethys subduction and collision. There are some traces of Palaeotethys along Baiburt-Sevanian terranes (Caucasus) (Gamkrelidze and Shengelia, 2007). Western Turkey is known as marking site of Palaeo- and Neotethys sutures. At the Karaburun Peninsula (west of Turkey), there are some granitoid intrusions with I-type affinity. They are 222-239 Ma old and are a result of Palaeotethys subduction (Erkül et al., 2008). The Paleotethys suture is traceable towards the east at the Sakarya, Mersin and Karakaya areas (Moix et al., 2008). Stampfli and Kozur (2006) believe that Karakaya fore arc basin had formed due to northward subduction of Palaeotethys. Also, some researchers believe that Palaeotethys subduction is southward (Şengör, 1979, 1990; Jassim and Goff, 2006; Ruban et al., 2007).

Despite a wealth of knowledge on Palaeotethys-related magmatism towards the east and west of Iran, there are limited publications on possible Palaeotethys-related granitoid magmatism in Iran. The Jurassic aged Lisar granite is located to the north of the suture in north Iran. Geochemical data and age dating of this spatially important granitoid will furnish more information on Palaeotethys evolution in Iran. This paper presents the petrography and whole rock geochemistry of this granite to describe geochemical features of the granite in relation with petrological processes and tectonic setting.

2. Geological Background and Local Geology

The study area is located within the West Alborz-Azerbaijan geological unit of Iran. It comprises a part of the Talesh Mountain range which is bounded to the west by Astara fault and Caspian Sea depression. The Alborz range represents late Precambrian to Eocene sedimentary and volcanic strata, which are intruded by Palaeozoic to Tertiary plutons and dikes (Annells et al., 1975, 1977; Stöcklin, 1974; Axon et al., 2001). This range marks a collision belt and is bounded by reverse faults characterized by southward dipping faults in the north and northward dipping faults in the south. Therefore the Alborz belt is *V*-shaped in N-S sections (Figure 1). The evolution of the Alborz belt mainly occurred in the Cenozoic (Rezaeian et al., 2012). Opening and subsequent closure of the Neotethys along the Zagros Mountains and opening of the Red Sea had important effects on the structural evolution of the Alborz belt (Axen et al., 2001; Guest et al., 2006; Omrani et al., 2013). Collision of the Gondwana-derived blocks with Eurasia occurred in the Late Triassic, resulting in the Eo-Cimmerian deformation in North Iran, followed by a strong but poorly known Neo-Cimmerian compression event in Middle-Late Jurassic times that mainly affected Central Iran (Zanchi et al., 2009). Structural and seismological data for the Alborz Range show that deformation is partitioned along parallel thrusts and left lateral strike-slip faults (Jackson et al., 2002; Allen et al., 2003; Ritz et al., 2006). Talesh Mountain, west of the Alborz Range (Figure 1), consists of

metamorphic rocks, granitoids, mafic, ultramafic rocks and sedimentary rocks that have a wide range of ages from Palaeozoic to Tertiary.

The Lisar area is a part of the Talesh Mountain range. The oldest rock units in the Talesh Mountains are pelitic schists and ultramafic rocks with Carboniferous to Permian age, which are exposed to the south of the Lisar area (not shown on the map of figure 2 but are indicated in the cross section, figure 2). Upper Cretaceous strata are andesite, dacite and tuffs, occasionally interlayered with shale and grey limestone. The finely laminated shales are dark and contain carbonaceous materials. Calcareous sandstone is other rock type in the Upper Cretaceous unit. The lowermost strata of the Paleogene units are made of a polygenetic conglomerate with Upper Cretaceous andesite, dacite, shale, limestone and some mafic volcanic rock fragments. It also contains pink-colour fragments of the Lisar granite (Figure 3a). This conglomerate is overlaying by andesitic tuffs, lava and brecciated lava. The dark limestone is cut by late light calcite veins. Veins also are found in Paleogene andesitic lavas. The andesitic lavas show mega-porphyric texture (with large plagioclase crystals) occasionally (Figure 3b). These rocks contain fragments of Lisar granite as xenoliths. The Neogene unit is mainly made of a polygenetic conglomerate and intercalated marl but the variation of fragment types is limited to limestone and volcanic fragments. In some parts it is consisted only from volcanic rock fragments (Figure 3c).

The Lisar granite appears as three separated outcrops (Asadian, 1999, Figure 2). It is emplaced and/or displaced along a north-south trending faults. Owing to very dense vegetation and soil coverage, it is not easy to determine the contacts of the granite, but it is in tectonic contact (strike slip fault) with Upper Cretaceous sandy limestone to the wet and is covered by Palaogene polygenetic conglomerate to the east. This granite appears as medium- to coarse-grained and pink coloured. K-feldspar, plagioclase, amphibole and quartz are visible in hand specimens. The granite samples appear as fresh rocks in the field which are hard to break by hammer. The Lisar granite appears as two distinct types in the field, the lighter granite and the darker one. The only difference is in the modal percentage of ferromagnetic minerals (mainly amphibole, see petrography section below). Microgranular mafic enclaves, which are similar to the main granite in mineralogy, can be seen in the field (Figure 3d). These are taken to represent rapidly cooled, fine-grained walls of the pluton, which are entered the solidifying magma. In some parts the Lisar granite is very fine-grained and appears with aplitic

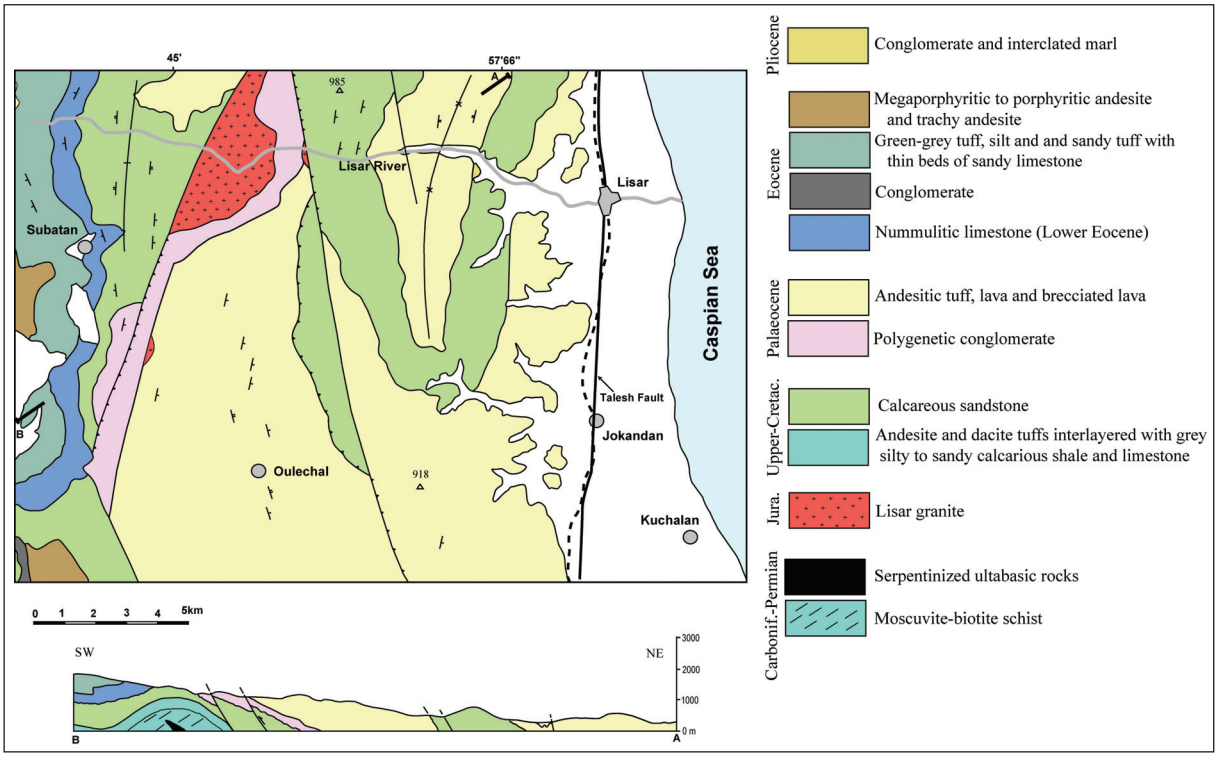

Figure 2- Simplified geological map of the Lisar area adapted from the 1:100000 scale geological map of Khalkhal (Asadian, 1999).

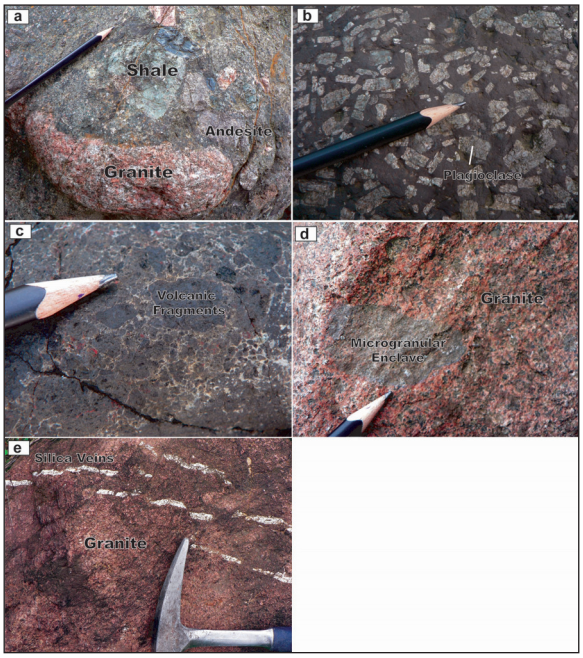

Figure 3- a) Paleogene conglomerate with Upper Cretaceous andesite, dacite, shale, limestone and some mafic volcanic rock, and Lisar granite fragments. b) Relatively large plagioclase in andesitic lavas. c) Neogene conglomerate consisted only from volcanic rock fragments. d) Microgranular dark enclaves, similar to the main granite in mineralogy within the main granite. e) Parallel silica veins in the Lisar granite showing an extensional regime during its emplacement.

texture. Parallel silica-rich aplitic veins in the Lisar granite (Figure 3e) point to extensional regime during emplacement of the granite and the later veins.

3. Study Methods

To study the Lisar granite, several rock samples were collected from the granite and the associated rocks. 60 thin sections were made from these rocks. Petrography studies were carried out by mineral composition and textural description of the samples. In order to study the geochemical features of the Liar granite, 11 optically well-defined representative samples among 60 investigated samples under the microscope were chosen for chemical analysis. These samples had the lowest alteration effects. The samples were crashed and pulverized by ZPS Ltd. in Tabriz, Iran. About 1 kg of each sample was crashed using a steel jaw crusher and then was pulverized to 200 mash or 75 micron. ~ 50 gr of each sample was packed in suitable plastic bags and were sent to Activation Laboratories in Ancaster, Canada for analysis. To analyse the samples for major, minor and trace elements, known amount of sample was mixed with lithium metaborate and were fused on gas heater. The resulted beads were used for XRF analysis of major oxides. They used for ICP-MS analyses after digestion in acid and needed dilution. International standards were used for calibrations. The uncertainties for major oxides in better than ±2% and for the minor and trace elements is better than 5%.

4. Petrography

The Lisar granite is red to pink in colour and appears as very hard rock in the field. However microscopic studies show that minerals, mainly feldspar, are altered. The rocks have different amphibole contents and are as relatively darker (with relatively more amphibole) and lighter (with relatively lower amphibole) granites. Except for amphibole content, there is no difference in mineralogy of these two types of granites under the microscope. The major minerals in the Lisar granite are K-feldspar (perthite and orthoclase), quartz, plagioclase (albite to oligoclase, based on optical properties), amphibole and biotite. The minor phases are zircon, apatite, titanite and opaque minerals. Chlorite (after biotite), sericite (after K-feldspar) and clay minerals (after plagioclase) are alteration products. The main textures are granular, perthite, poikilitic and intergrowth micrographic textures (Figure 4). Quartz appears as xenomorphic crystals and micrographic texture appears at the margin of large plagioclase crystals. Amphiboles are dark green to brown pleochroic hornblende, which occurs as crystals among other minerals and as inclusions in large perthitic K-feldspar. Amphibole crystals show accumulation in some parts of the rock resembling cumulate texture. Biotite, which is less abundant than hornblende, is altered to chlorite along cleavage. The granophyre texture in some samples points to eutectic crystallization of quartz and feldspar in these rocks. Some samples from the Lisar granite show slight deformation and also cataclastic textures. Small crushed crystals of quartz can be seen along with larger quartz crystals in the samples with cataclastic texture. Estimation of mineral modal percentages was made by investigation of thin sections under the microscope and plagioclase, K-feldspar and quartz contents were plotted on Streckeisen diagram (Figure 5). All samples are granite according to this diagram.

The Lisar granite samples are very similar to some A-type granites in the world such as Krajaa granite in Finland (Juravanen et al., 2005), Gebel Musa A-type

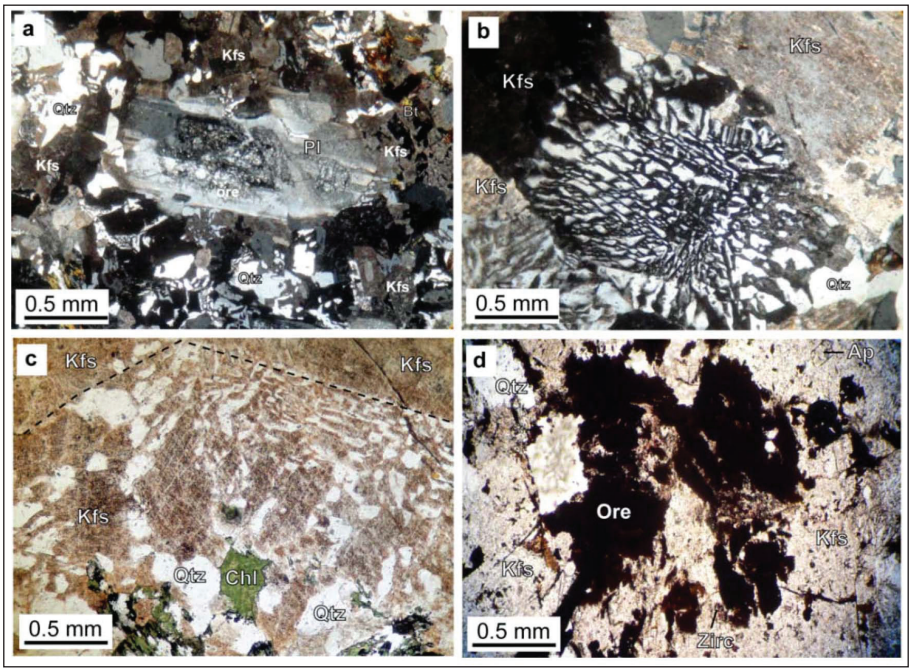

Figure 4- Petrographical features of the Lisar granite a) K-feldspar, plagioclase and quartz are the main mineral phases in the Lisar granite. b) Graphic texture in the Lisar sample. c) K-feldspar as the main mineral and d) Apatite and opaque minerals in the rock.

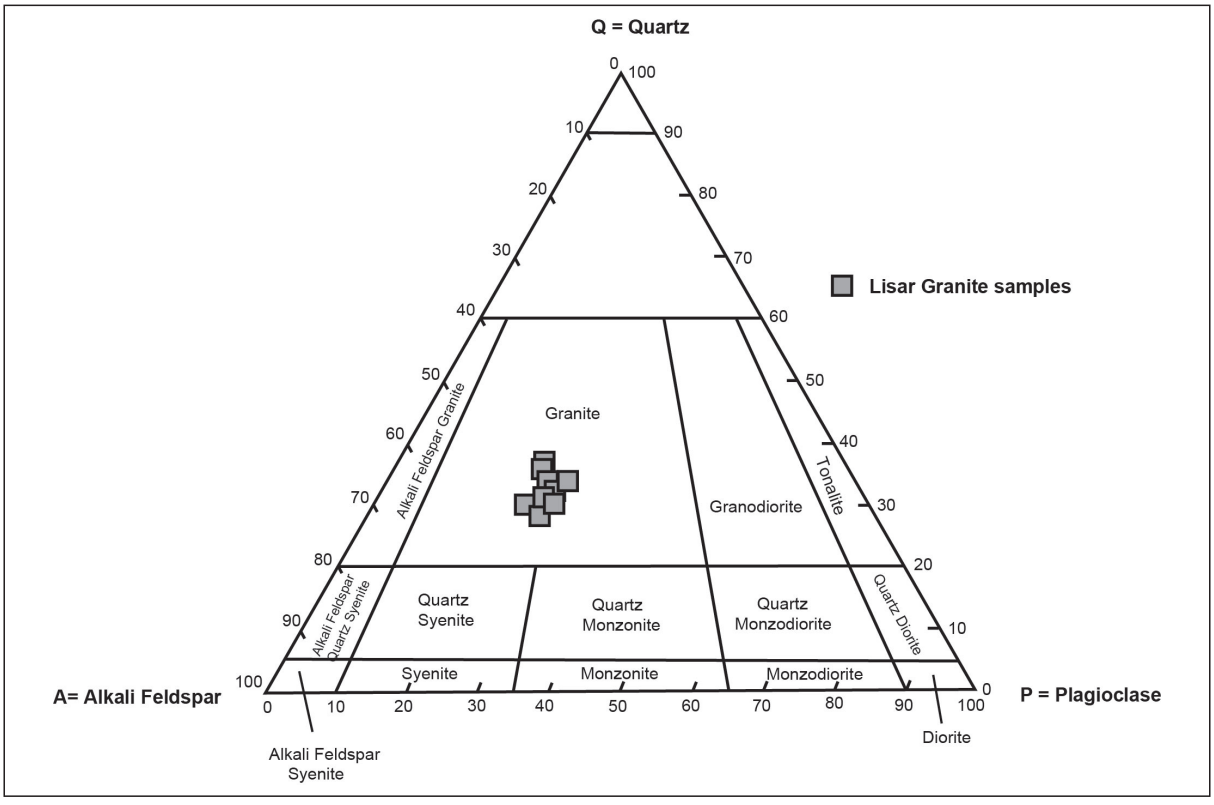

Figure 5- Streckeisen diagram for the studied samples indicating granite mineral composition for the rocks.

granite from Egypt (Katzir et al., 2006), pink A-type granites from Rajestan, India (Kaur et al., 2007) and Mianning A-type granite from south China (Huang et al., 2008). All these A-type granites are formed from predominant K-feldspar (mainly as perthite), quartz and subordinate amounts of plagioclase. They may contain biotite and hornblende. The Lisar granite is K-rich, therefore Na-rich phases such as Na-amphibole (e.g. riebeckite) are not present in the samples.

5. Whole Rock Geochemistry

Table 1 includes the major oxide contents and normative mineralogical composition and table 2 contains the minor and trace element contents of the analysed samples.

All samples from Lisar granite plot in the granite and alkali granite fields on the plot of De La Roche et al. (1980) (Figure 6a). On diagram of Th versus Co (after Hastie et al., 2007), the analysed samples show high K calc-alkaline and shoshonitic nature for the original magma (Figure 6b).

The parental magma had high K content (Figure 6b, Hastie et al., 2007), was either I or A-type (Figure 6c) and mainly of metaluminous to peraluminous nature (Figure 6d). The samples are ferroan and mainly alkaline on the diagrams of Frost et al. (2001) (Figure 7). The Lisar granite has A-Type geochemical feature, such as high Ga/Al ratios, elevated concentration of HFSE (e.g. Zr, Nb and Y), low CaO, MgO, Cr, Co, Ni, Sr and Eu contents as compared to S- and I-type granitoids (Whalen et al., 1987; Eby, 1990; Frost et al., 2001). Using Whalen et al. (1987) diagrams (Figure 8), an A-type affinity is evident for the studied samples. On REE diagram normalized to chondrite values (Figure 9a), Lisar granite samples show a distinct negative Eu anomaly. A decrease from LREE content to HREE content is visible. These features

Table 1- Major oxides and CIPW norm mineral composition of Lisar granite samples.

Sample	RB4	RB39	RB12	RB5B	RB8	RB6	RB13	RB20	RB9	RB38	RB7
Major Axides wt%											
SiO_2	72.08	71.78	72.13	65.95	67.93	66.72	65.87	64.41	64.85	67.77	68.11
TiO_2	0.33	0.31	0.42	0.60	0.71	0.67	0.62	0.65	0.71	0.52	0.64
Al_2O_3	12.9	12.21	12.46	13.92	14.05	13.96	13.85	13.96	13.73	14.32	13.98
$Fe_2O_3^T$	2.54	2.33	2.74	5.17	5.38	5.27	5.19	5.39	5.28	3.68	3.49
MnO	0.04	0.04	0.05	0.11	0.11	0.10	0.10	0.12	0.11	0.06	0.05
MgO	0.13	0.11	0.13	0.42	0.54	0.63	0.48	0.64	0.71	0.49	0.53
CaO	0.64	0.69	0.66	1.78	1.63	1.53	1.86	2.58	2.62	1.34	1.22
Na_2O	3.48	3.75	3.46	4.65	4.13	4.39	4.58	3.79	4.01	4.04	4.12
K_2O	5.25	5.86	5.38	3.8	3.58	3.73	3.66	3.92	3.88	4.69	4.87
P_2O_5	0.03	0.04	0.04	0.14	0.14	0.11	0.12	0.18	0.17	0.14	0.15
LOI	1.29	1.64	1.71	1.8	1.84	1.69	1.74	3.03	3.16	1.78	1.86
Total	98.71	98.76	99.18	98.34	100.04	98.80	98.07	98.67	99.23	98.83	99.02
CIPW Norm, wt%											
Quartz	30.264	27.049	30.013	20.752	26.303	23.002	21.296	21.846	21.321	23.114	22.526
Corundum	0.400	0.00	0.00	0.00	0.752	0.182	0.00	0.00	0.00	0.496	0.072
Orthoclase	31.026	34.631	31.794	22.451	21.157	22.043	21.629	23.166	22.930	27.716	28.780
Albite	29.447	30.177	29.278	39.347	34.947	37.147	38.755	32.070	33.932	34.185	34.862
Anorthite	2.979	0.00	2.577	5.886	7.172	6.872	6.422	9.501	8.004	5.733	5.073
Hypersthene	0.324	0.00	0.324	0.916	1.345	1.569	1.102	1.479	1.101	1.230	1.320
Ilmenite	0.077	0.094	0.105	0.231	0.242	0.218	0.220	0.259	0.242	0.139	0.111
Hematite	2.540	2.857	2.740	5.170	5.380	5.270	5.190	5.390	5.280	3.680	3.490
Titanite	0.00	0.630	0.307	1.177	0.00	0.00	1.242	1.271	1.433	0.00	0.00
Rutile	0.286	0.00	0.235	0.00	0.584	0.550	0.00	0.00	0.00	0.443	0.580
Apatite	0.071	0.095	0.095	0.332	0.332	0.261	0.284	0.426	0.403	0.332	0.355
Total	97.414	97.123	97.467	96.548	98.213	97.114	96.343	95.656	96.085	97.059	97.169

Table 2- Rare earth and trace elements contents of the studied samples (all in ppm).

Sample	RB4	RB39	RB12	RB5B	RB8	RB6	RB13	RB20	RB9	RB38	RB7
Sc	3	4	4	11	9	11	8	11	11	8	10
Be	4	3	4	3	2	3	2	3	2	3	2
V	17	15	15	25	27	25	26	32	30	30	28
Ba	558	633	537	592	612	588	603	685	703	730	741
Sr	47	42	44	106	98	95	111	102	106	110	112
Y	62	69	65	63	65	64	63	56	58	49	46
Zr	430	455	415	416	427	420	423	302	312	416	420
Co	2	1	1	4	3	3	1	6	4	4	4
Cu	70	112	86	70	68	75	91	170	166	60	57
Zn	40	61	52	90	94	98	87	100	98	60	69
Ga	20	18	21	21	17	19	22	21	20	20	21
Ge	2	1	1	2	1	1	1	2	2	1	1
Rb	209	212	227	126	119	123	115	141	139	151	158
Nb	15	13	15	22	25	23	25	18	17	19	18
Mo	4	5	4	4	5	4	5	5	4	2	2
Ag	1	0.7	0.8	0.5	0.4	0.7	0.6	<0.5	<0.5	<0.5	<0.5
Sn	9	8	11	6	7	12	8	8	7	7	9
Sb	<0.5	<0.5	<0.5	0.6	0.7	0.6	<0.5	1.2	1.1	0.7	0.6
Cs	3.4	4.1	3.7	2	2	2	1	2.6	2.5	3.6	3.4
La	65.9	64.6	65.4	51.5	55.4	52.7	51.9	56.3	55.8	51.2	52.3
Pr	13.1	14.3	12.5	11.9	12.1	11.8	12.2	11.7	11.8	11.1	11.2
Nd	44.8	45.69	44.6	45.6	45.7	46.1	45.4	44.9	50.6	41.8	40.9
Sm	9	8	8	9.9	9.6	9.8	9.6	9.3	9.1	8.8	8.9
Eu	0.61	0.77	0.69	1.92	1.89	1.97	1.93	1.61	1.48	1.44	1.28
Gd	8.2	8.1	7.8	10.1	10.8	10.4	10.2	8.7	8.6	8.4	8.3
Tb	1.5	1.6	1.4	1.8	1.7	1.8	1.8	1.5	1.3	1.4	1.3
Dy	10.3	10.2	10.7	11.1	11.4	11.3	11.1	9.7	9.8	9	8
Ho	2.2	3.1	2.8	2.3	2.4	2.4	2.5	2	2	1.8	1.8
Er	6.6	6.4	6.3	6.9	6.3	6.8	6.9	5.9	5.3	5.3	5.7
Tm	1.07	1.12	1.23	1.06	1.07	1.12	1.08	0.9	0.7	0.81	0.82
Yb	7.4	8.1	7.3	7	8	7	7	6	6	5.6	5.9
Lu	1.11	1.09	1.16	1.06	1.07	1.06	1.06	0.95	0.91	0.84	0.79
Hf	11.6	10.8	11.2	8	9.1	8.3	8.1	5.8	5.7	7.7	7.5
Ta	1.7	1.6	1.4	1.7	1.8	1.8	1.8	1.4	1.2	1.4	1.3
W	2	4	2	1	4	3	3	3	3	<1	<1
Tl	0.6	0.5	0.6	0.5	0.5	0.4	0.5	0.5	0.4	0.5	0.4
Pb	18	17	18	19	17	19	18	24	25	14	15
Th	24.9	25.2	24.6	13.1	13.3	13.3	13.1	15.4	15.1	15.6	15.4
U	6.3	6.5	6.3	3.5	3.7	3.4	3.7	3.2	3.3	1.8	1.9

are characteristic of A-type granites (e.g. Obbnäs rapakivi A-type granite from Finland, Jurvanen et al., 2005). Lisar samples have low Nb (13–25 ppm), high Sr (42–112 ppm) and moderate Rb (115–227 ppm) concentrations. The chondrite-normalized REE diagram (Figure 9a) shows that the Lisar samples are LREE enriched with a flat HREE and negative Eu anomaly. This indicates the removal of plagioclase by fractional crystallization. Negative anomalies in Ba, Sr, and Eu, as shown in the primitive mantle-normalized trace element and REE diagrams (Figure 9b), testifies for fractional crystallization of feldspar while Nb, Ta, Zr and Hf are not depleted, implying little contribution of subduction-related components in the magma source of Lisar granite. The depletion of Ti coupled with high Nb and Ta concentrations suggests crystallization of Fe-Ti oxides as the main Ti-bearing phase, with little influence of rutile or titanite. Rutile and titanite usually have high concentrations of Nb and Ta (Manning and Bohlen 1991; McDonough 1991; Green 1995; Rudnick et al. 2000; Foley et al. 2002). Ilmenite usually has much lower Nb and Ta (Ding et al. 2009). Therefore, crystallization of Fe-Ti oxide (more likely ilmenite) consumed Ti, leading to depletion of Ti in the resulted granite without significant decrease of Nb and Ta. The decrease in Sr

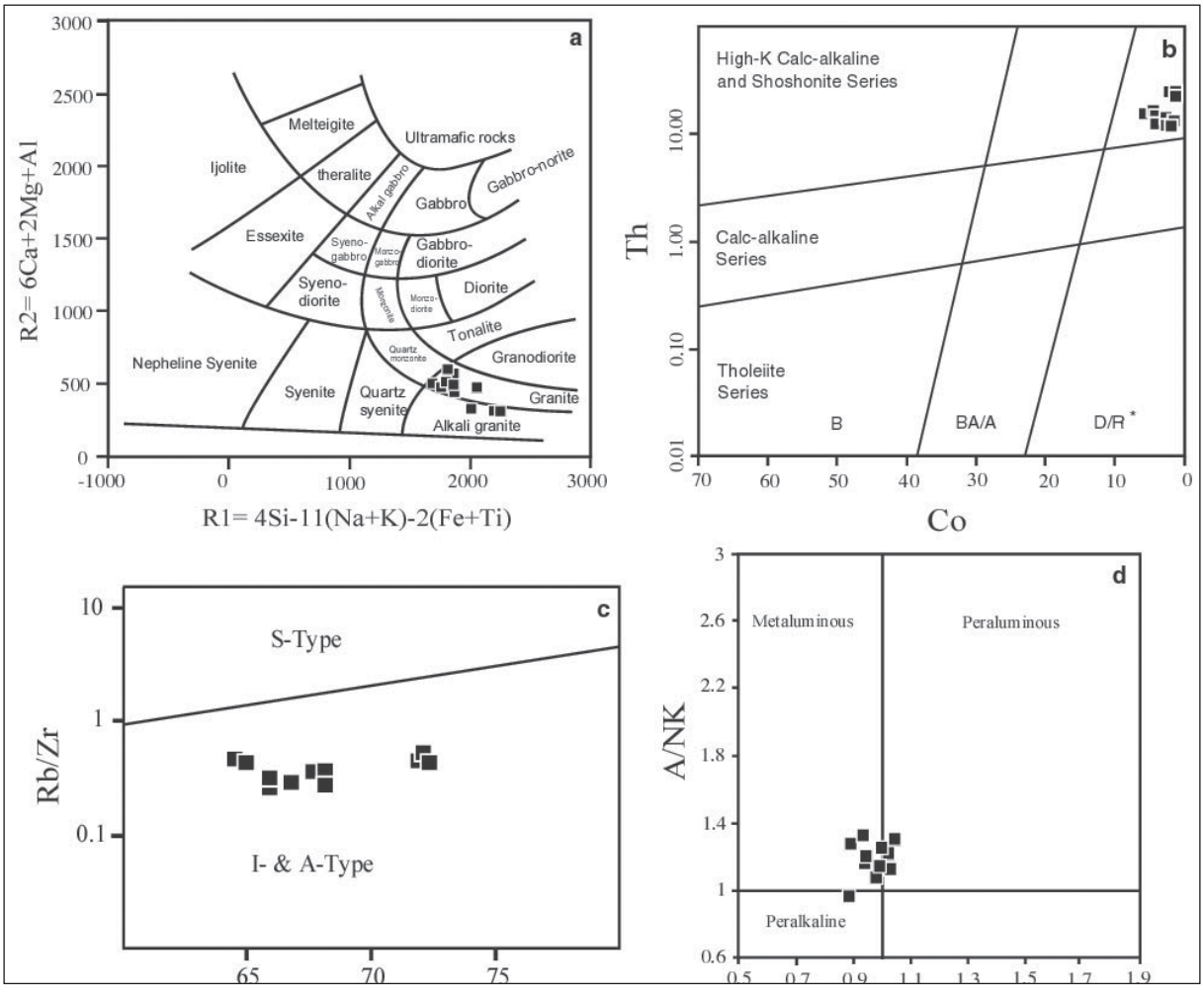

Figure 6- a) Classification of granites according to De La Roche et al. (1980). The samples plot in the granite and alkali granite fields. b) Th vs. Co diagram of Hastie et al. (2007) indicates high K calc-alkaline magma for the Lisar granite. c) The studied rocks have either I or A-type nature. d) The original magma had metaluminous to peraluminous characteristic on A/NK versus ASI diagram.

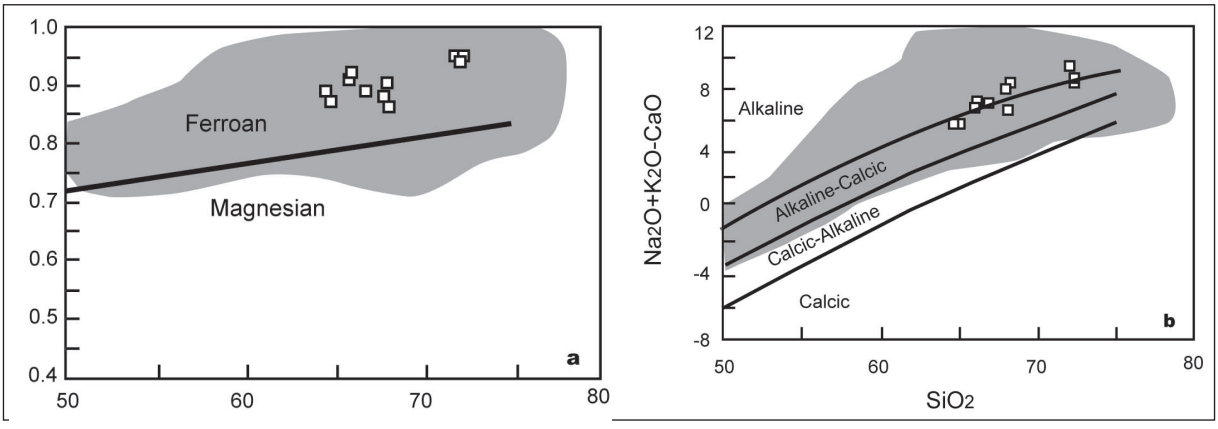

Figure 7- Ferroan (a) and mainly alkaline nature (b) for the Lisar samples on the diagrams from Frost et al. (2001).

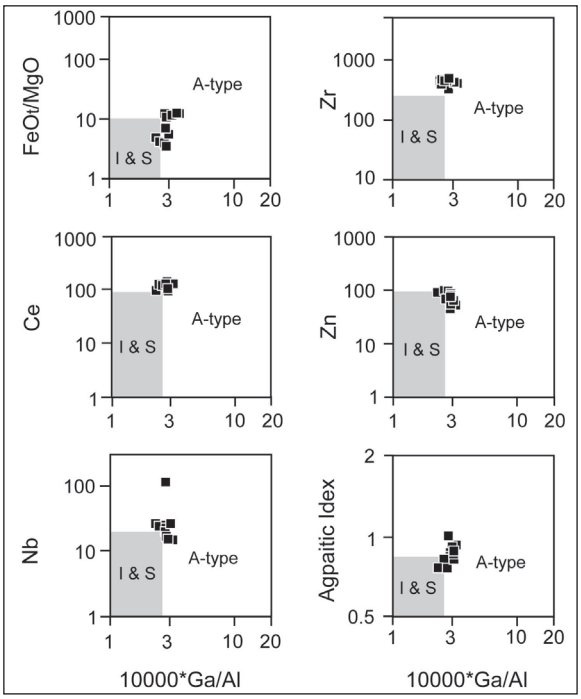

Figure 8- Determination of granite type according to trace elements and agpaitic index (Whalen et al., 1987). The Lisar granite is A- type according to these diagrams.

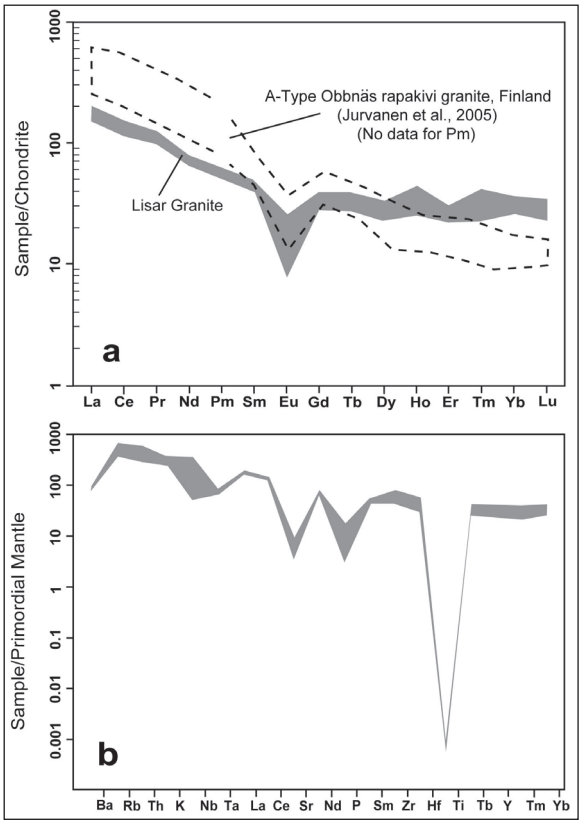

Figure 9- a) Trace elements contents of the studied samples normalized to chondrite (normalizing values from Sun and McDonough, 1989). Trace element pattern for Obbnas rapakivi granite (Jurvanen et al., 2005) is provided for comparison. b) Element content normalized to primordial mantle. Distinct Eu, Ti, P and Sr is obvious.

and Ba and slight increase in Rb with increasing SiO_2 may also be due to plagioclase fractionation (Figure 10).

Based on the trace element contents of the rocks, amphibole and plagioclase crystallization was the main factor controlling the rock composition and fractional crystallization. According to Watson and Harrison (1984) the amount of dissolved phosphorus (and Zr) can be used to estimate the granitic magma crystallization temperature. Apatite was found as small needle-like inclusions in other minerals in the

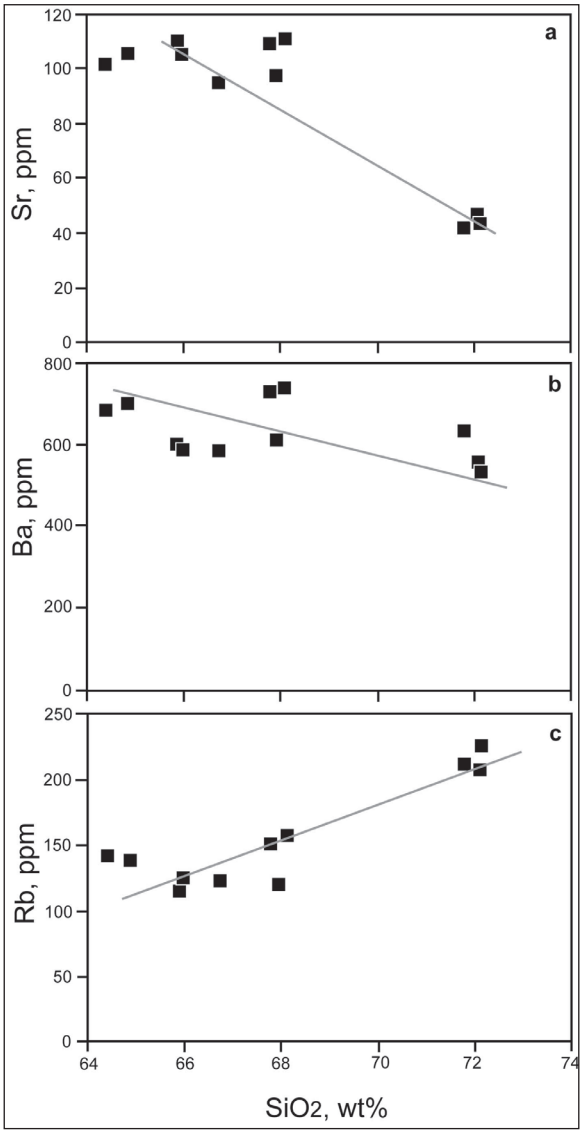

Figure 10- Variation diagrams for Sr, Ba and Rb versus SiO_2 for the Lisar samples. Decreasing of Sr and Ba and slight increasing of Rb contents are in agreement with plagioclase fractionation as a controlling factor in the Lisar granite generation.

Lisar granite. According to P_2O_5 versus SiO_2 diagram of Watson and Harrison (1984), The Lisar granite was crystallized at temperatures about 800 to 900°C (Figure 11). These temperatures are close to liquidus temperatures estimated for A-type melts at 5 kbar (Shkodzinsky, 1985). Some samples with lower temperatures on this diagram may show samples with low modal apatite content. Nb-Y-3Ga triangular diagram of Eby (1992) shows that the studied samples are of A_2 subgroup (Figure 12). On the discrimination diagrams of Pearce (1996) Lisar samples fall in the within plate granites (Figure 13a). On SiO_2 versus Al_2O_3 diagram of Maniar and Piccolli (1989) the samples plot mainly in the post orogenic field (Figure 13b).

6. Discussion

A-type granites occur in diverse tectonic settings including oceanic islands, continental rifts, extensional parts of the continental crust, stable continental crust and post orogenic environment. These type of granite may form as non-orogenic (during continental rifting) and post-orogenic intrusions during extensional régime (Sylvester, 1989). Therefore two main types of A-type granites are non-orogenic and post-orogenic granites. Post orogenic granites tend to have more crustal components. A_1 subgroup of A-type granites (Eby, 1992) are similar to oceanic island rocks in overall composition, while A_2 subgroup are similar to average of composition of oceanic rocks and mean crustal composition. A_1 subgroup occurs mainly during rifting within the plates and is usually accompanied by mafic rocks as a result of plume or hot spot activities, while A_2 subgroup represents post-collision events (Eby, 1992).

Different possibilities for generation of A-type granitic melts are proposed. Some are summarized below. Re-melting of granitic melts containing quartz, plagioclase and K-feldspar, which have experienced at least one melting event already (Collins et al., 1982; Clemens et al., 1986; Whalen et al., 1987) is a possible source for A-type granitic melts. This possibility is argued by Creaser et al. (1991) and Landenberger and Collins (1996). Partial melting of dehydrated lower crust, resulted as residua from fractionation of I-type magma at temperatures exceeding 900°C in a subduction-related environment (Landenberger and Collins, 1996) is proposed instead. However Creaser et al. (1991) stated that partial melting of such a residua cannot provide chemical features of A-type granites. They proposed partial melting of tonalitic to granodioritic crust for generation of A-type granitic magma. Taylor et al. (1981) and Harris et al. (1986) consider the per-alkaline nature of non-orogenic A-type granites as a result of CO_2 and halogen-rich fluid metasomatism during emplacement or later events. Whalen et al. (1987) believe that highly dehydrated alkaline phase and low CO_2 content of these types of rocks is in contradiction with this hypothesis. As it is evident there is not a consensus for the origin of A-type granite magmas but some observations on Yb/Ta and Y/Nb ratios for A-type granites (White Mountain, Eby, 1992) show that they are related to silica under saturated mafic rocks. These mafic rocks can be directly related to silica-rich highly fractionated rocks (A-type granites). This may

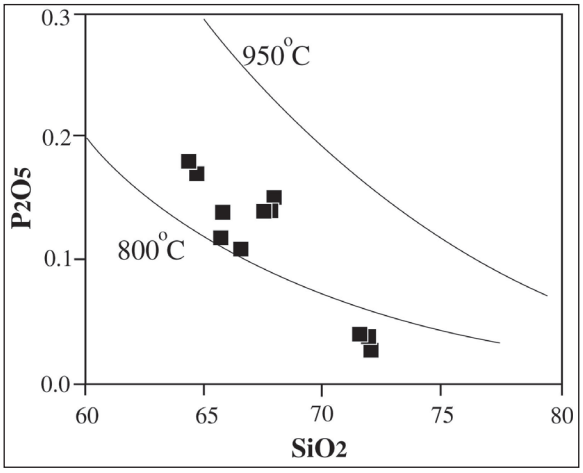

Figure 11- According to P_2O_5 versus SiO_2 diagram of Watson and Harrison (1984), The Lisar granite was crystallized at temperatures about 800 to 900°C.

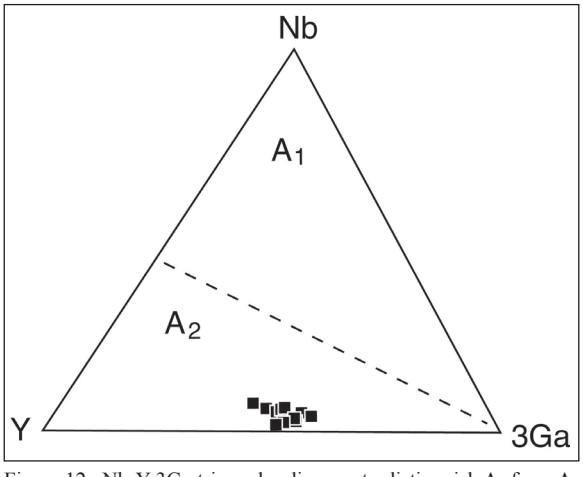

Figure 12- Nb-Y-3Ga triangular diagram to distinguish A_1 from A_2 granites (Eby, 1992). The studied samples are of A_2 sub-group.

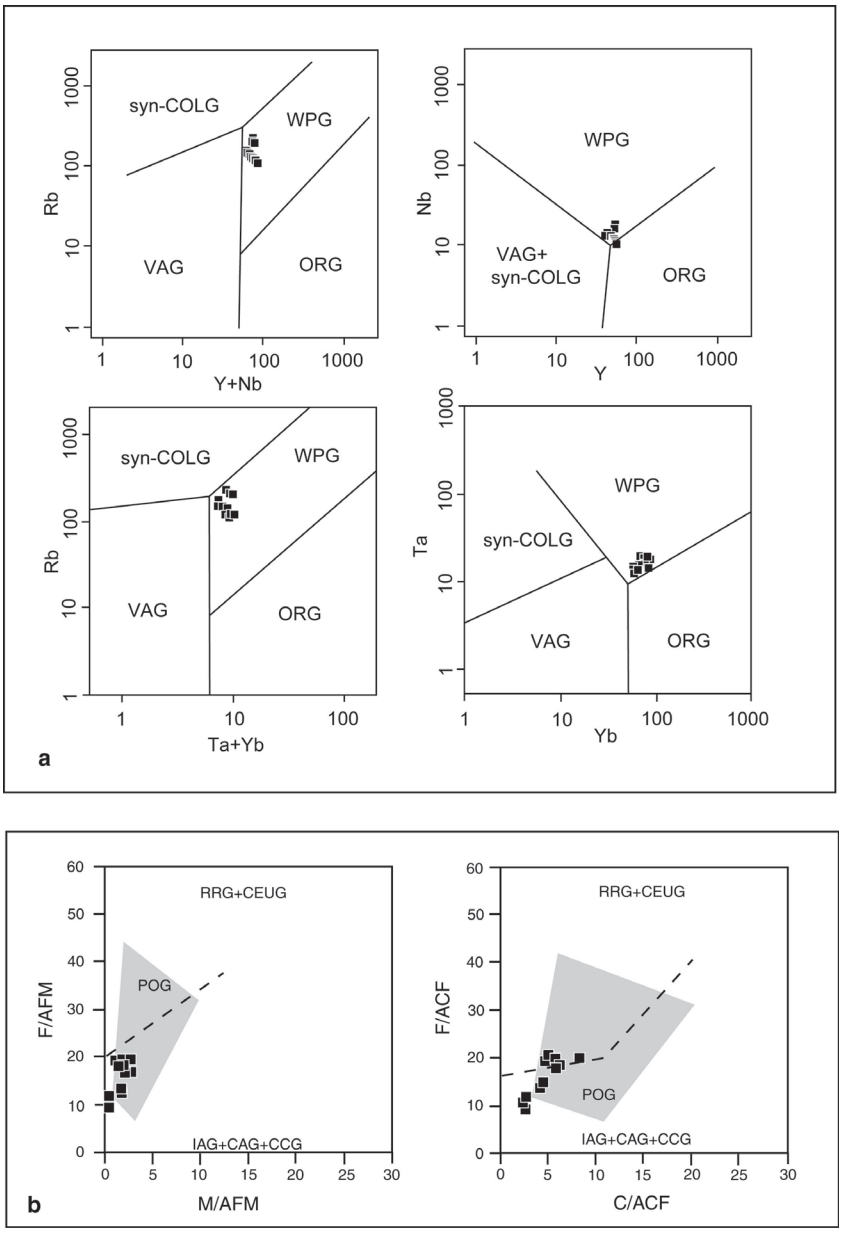

Figure 13- a) Within plate nature for the studied samples on discrimination diagrams of Pearce at al. (1984). b) Diagrams of Maniar and Piccolli indicate a post-collision setting for the Lisar granite.

testify to mantle origin for at least some of the A-type granites.

It is difficult to consider a single source as origin for the Lisar granite magma unequivocally. Some chemical features of Lisar granites show that they could have been originated from a crustal source, which may have been affected by the mantle materials (e.g. Ce/Pb versus MgO content, Figure 14). The studied samples show high SiO_2 (>64 wt%) and low MgO (<0.71wt%) and TiO_2 (<0.31 wt%) concentrations. This suggests that the original magma was not directly derived from a mantle source. There are not mafic or intermediate igneous rocks contemporarily associated with the Lisar granite. This, rules out its formation from a directly mantle-derived magma. Since extensive fractional crystallization (Peccerillo et al., 2003; Shellnutt et al., 2009) generates considerable amounts of mafic rocks, which is not the case for the Lisar granite. Mafic volcanic rocks of the area are much younger than Lisar granite. Major and trace element contents of the studied samples are more compatible with a lower

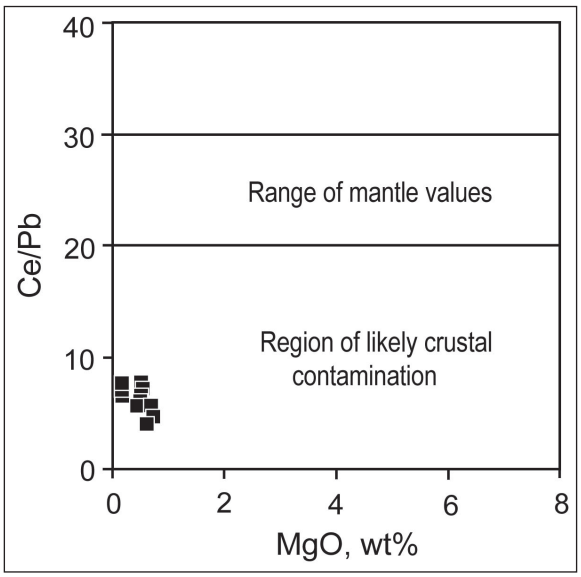

Figure 14- Ce/Pb versus MgO diagram for the studied rocks which shows crustal materials contribution in genesis of Lisar granite magma.

continental crust origin with possible some limited mantle source contribution for this granite.

Bonin (2007) considers some geochemical characteristics for A-type granites. This granites have Zr+Nb+Ce+Y>350. The sum of these trace elements is above 376 ppm for all samples from the Lisar granite. According to Bonin (2007) Y/Nb ratio for A_1 subgroup is <1.2 while it is >1.2 for A_2 subgroup. This ratio for the Lisar granite is 2.52 to 5.31, compatible with A_2 subgroup. In terms of tectonic environment, considering the studied granite of A_2 subgroup, it is formed more likely in an extensional post-orogenic setting. This is verified by the field observations (parallel veins within the granite) and chemical properties. Recently Madanipour et al. (2015) dated one sample of Lisar granite (U/Pb on zircon) and reported a 179±18 Ma concodria age. This age is corresponding to Late Jurassic. Therefore Lisar granite represents Cimmerian post-collision magmatism in north Iran following closure of Palaeotethys ocean and subsequent collision.

Conclusions

Most researchers believe that the continuation of the Palaeotethys suture from China into west Turkey can be traced in North Iran along the Alborz Mountains (Alavi, 1991; Omrani et al., 2013, Shafaii Moghadam et al., 2015). This opinion is debated and other researchers consider the continuation of Palaeotethys to the north and outside of the Iranian crust (Zanchetta et al., 2009). Study of Palaeotethys ophiolites and high pressure rocks (eclogites and blueschists) helps to work out the location of this suture in northern Iran (Zanchetta et al., 2009; Omrani et al., 2013; Shafaii Moghadam et al., 2015). Granitoids play an important role in this regard and study of granitoid plutons at different tectonic settings can help to reconstruct the geodynamic evolution of the Palaeotethys Ocean (Majidi, 1975; Debon et al., 1987; Erkül et al., 2008; Hennig et al., 2009). In the Talesh Mountain at the western continuation of the Alborz range, the Lisar granite occurs with tectonic contacts with Upper Cretaceous sandy limestone, which is covered by Paleogene polygenetic conglomerate. Based on petrography studies the main minerals are abundant coarse-gained K-feldspar, quartz, plagioclase, biotite and amphibole. This proposes A-type for the Lisar granite. Based on whole rock geochemistry, the Lisar granite has derived from a high K magma and is A-type in nature, belonging to A_2 subgroup. The samples are characterized by negative Eu anomaly and a decrease from LREE to HREE contents. More likely the original magma forming the Lisar granite generated from partial melting of a lower continental crustal source with possible contribution from the mantle materials. Considering the already published age of Late Jurassic for the Lisar granite by Madanipour et al. (2015) using U/Pb method on zircon, this granite represents Cimmerian post-collision magmatism in north Iran following closure of Palaeotethys Ocean and subsequent collision.

Acknowledgements

We would like to thank kind people of Lavandaville village for their hospitality during our field works and our stay in north Iran. Mrs. Nassrin R. Saadat form ZPS Ltd. Iran is acknowledged for her helps with analyses arrangement. Generous helps from Cahit Dönmez and Taner Ünlü during preparation of the manuscript are highly appreciated. We are grateful to Dr. Mehmet Arslan and an anonymous reviewer for their perceptive reviews and detailed comments.

References

Alavi, M. 1991. Sedimentary and Structural characteristics of the Paleo-Tethys remnants in northeastern Iran. Geological Society of America Bulletin 103, 983-992.

Allen, M.B., Ghassemi, M.R., Shahrabi, M., Qorashi, M. 2003. Accommodation of late Cenozoic shortening in the Alborz range, northern Iran. Journal of Structural Geology 25, 659–672.

Annells, R.N., Arthurton, R.S., Bazley, R.A., Davies, R.G. 1975. Explanatory text of the Qazvin and Rasht quadrangles map: Tehran, Geological Survey of Iran, 94 p.

Annells, R.N., Arthurton, R.S., Bazley, R.A., Davies, R.G., Hamedi, M.A.R., Rahimzadeh, F. 1977. Geological map of Iran, Shakran sheet 6162: Geological Survey of Iran, scale 1:100 000.

Asadian, O. 1999. Geological map of Khalkhal, 1:100000. Geological Survey of Iran.

Axen, G. J., Patrick, S.L., Marty, G., Stockli, D., F., Hassanzadeh, J. 2001. Exhumation of the west-central Alborz Mountains, Iran, Caspian subsidence, and collision-related tectonics. Geology 29.6, 559-562.

Berberian, F., Berberian, M. 1981. Tectono-plutonic episodes in Iran. In: H. Gupta and F. Delany (Editors), Zagros- Hindu Kush-Himalaya Geodynamic Evolution. American Geophysical Union, Geodynamic Series 3, 5-32.

Bonin, B. 2007. A-type granites and related rocks: evolution of a concept, problems and prospects. Lithos 97,1–29.

Boulin, J. 1981. Afghanistan structure. Greater India concept and eastern Tethys evolution. Tectonophysics 72, 261-287.

Clark, G.C., Davies, R.G., Hamzepour, G., Jones, C.R. 1975. Explanatory text of Bandar-e-Anzali quadrangle map, 1:250,000. Geological Survey of Iran.

Clemens, J. D., Hollaway, J. R., White, A. J. R. 1986. Origin of an A-type granite: experimental constraints. American Mineralogist 71, 317-324.

Collins, W.J., Beams, S.D., White, A.J.R., Chappell, B.W. 1982. Nature and origin of A-type granites with particular reference to southeastern Australia. Contributions to Mineralogy and Petrology 80, 189–200.

Creaser, R.A., Price, R.C., Wormald, R. J. 1991. A-type granites revisited: Assessment of a residual-source model. Geology 19, 163–166.

Debon, F., Afzali, H., LeFort, P., Sonet, J., Zimmermann, J.L. 1987. Plutonic rocks and associations in Afghanistan: typology, age and geodynamic setting. Memoire Science de la Terre, Nancy 49, 132 pp.

Delaloy, M., Jenny, J., Stampfli, G. 1981. K-Ar dating in the eastern Elburz (Iran). Tectonophysics 79, 27-36.

De La Roche, H., Leterrier J., GrandIauale, P., Marcher, M. 1980. A classification of volcanic and plutonic rocks using R_1- R_2 diagrams and major element analysis. Chemical Geology 183-210.

Ding, X., Lundstrom, C., Huang, F., Li, J., Zhang, Z.M., Sun, X.M., Liang, J.L., Sun,W.D. 2009. Natural and experimental constraints on formation of the continental crust based on niobium–tantalum fractionation. International Geology Review 51, 473–501.

Eby, G. N. 1990. The A-Type granitoids: A Review for their occurrence and characteristics and speculations on their petrogenesis. Lithos 26, 115-134.

Erkül, A., Sözbilir, R., Erkül, F., Helvaci, C., Ersoy, Y., Sümer, Ö. 2008. Geochemistry of I-type granitoids in the Karaburun Peninsula, West Turkey: Evidence for Triassic continental arc magmatism following closure of the Palaeotethys. Island Arc 17, 394–418.

Foley, S., Tiepolo, M., Vannucci, R. 2002. Growth of early continental crust controlled by melting of amphibolite in subduction zones. Nature, 417, 837–840.

Frost, B. R. , Arculus, R. J. , Barnes, C. G. , Collins, W. J., Ellis, D. J., Frost, C. D. 2001. A geochemical classification of granitic rock suites. Journal of Petrology 42, 2033 – 48.

Gamkrelidze, I.P., Shengelia, D.M. 2007. Pre-Alpine geodynamics of the Caucasus, suprasubduction regional metamorphism and granitoid magmatism. Bulletin of the Georgian national academy of sciences 175.

Ghavidel-Syooki, M. 2007. Palynostratigraghy and Palaeogegraphy of the Gorgan schists in southern Gorgan city (southeastern Caspian Sea), eastern Alborz range, northern Iran. CIMP Lisbon Abstracts 63-64.

Green, T.H. 1995. Significance of Nb/Ta as an indicator of geochemical processes in the crust-mantle system. Chemical Geology 120, 347–359.

Guest, B., Axen, G.J., Lam, P.S., Hassanzadeh, J. 2006. Late Cenozoic shortening in the west-central Alborz Mountains, northern Iran, by combined conjugate strike slip and thin-skinned deformation. Geosphere 2/1, 35–52.

Harris, N.B.W., Marzouki, F.M.H., Ali, S. 1986. The Jabel Sayid Complex, Arabian Shield: geochemical constraints on the origin of peralkaline and related granites. Journal of the Geological Society of London 143, 287- 295.

Hastie, A. R., Kerr, A. C., Pearce, J. A., Mitchell, S. F. 2007. Classification of Altered Volcanic Island Arc Rocks using Immobile Trace Elements: Development of the Th–Co Discrimination Diagram. Journal of Petrology 48, 2341-2357.

Hennig, D., Lehmann, B., Frei, D., Belyatsky, B., Zhao, X.F., Cabral, A.R., Zeng, P.S., Zhou, M.F., Schmidt, K. 2009. Early Permian seafloor to continental arc magmatism in the eastern Paleo-Tethys: U-Pb age and Nd-Sr isotope data from the southern Lancangjiang zone, Yunnan, China. Lithos 113, 408-422.

Huang, X.L., Xu, Y.G., Li, X.H., Li, W.X., Lan, J.B., Zhang, H.H., Liu, Y.S., Wang, Y.B., Li, H.Y., Luo, Z.Y., Yang, Q.J. 2008. Petrogenesis and tectonic implications of Neoproterozoic, highly fractionated A-type granites from Mianning, South China. Precambrian Research 165(3), 190-204.

Jackson, J., Priestley, K., Allen, M., Berberian, M. 2002. Active tectonics of the South Caspian Basin. Geophysical Journal International 148, 214–245,

Jassim, S. Z., Goff, J. C. 2006. Geology of Iraq. Dolin, Prague and Moravian Museum Brno. 338p.

Jurvanen,T., Elkund, O., Väisänen, M. 2005. Generation of A-type granitic melts during the late Svecofennian metamorphism in southern Finland. GFF 127, 139–147.

Katzir, Y., Eyal, M., Litvinovsky, B. A., Jahn, B. M., Zanvilevich, A. N., Valley, J. W., Beeri, Y., Pelly, I., Shimshilashvili, E. 2007. Petrogenesis of A-type granites and origin of vertical zoning in the Katharina pluton, Gebel Mussa (Mt. Moses) area, Sinai, Egypt. Lithos, 95(3), 208-228.

Kaur, P., Chaudhri, N., Paczek, I., Kroner, A., Hofmann, A. W. 2007. Geochemistry, zircon ages and whole rock Nd isotopic systematics for the Palaeoproterozoic A-type granitoids in the northern part of the Delhi belt, Rajasthan, NW India: implications for late Palaeoproterozoic crustal evolution of the Aravalli craton. Geological Magazine 144(2), 361-378.

Landenberger, B., Collins, W.J. 1996. Derivation of A-type Granites from a Dehydrated Charnockitic Lower Crust: Evidence from the Chaelundi Complex, Eastern Australia. Journal of Petrology 37, 145–170.

Madanipour, S., Ehlers, T. A., Yassaghi, A., Enkelmann, E. Siebel, W. 2015. Time-temperature U-Th-Pb-He modelling of the Lisar Granite in the Talesh Mountains,Evidence for Late Cenozoic exhumation pattern at NW Iranian Plateau. The first meeting of Tectonic and Structural Geology Association of Iran, Tehran.

Majidi, B. 1987. The geochemistry of ultrabasic and basic lava flows occurrences in northeastern Iran, In Geodynamic project in Iran. Geological Survey of Iran, Report No. 51,463-477.

Majidi, B. 1991. Ètude structurale de là region de Mashad (Iran). Les problemes des metamorphites, serpentinites et granitoides hercyniens. These de Docteur Ingenieur,Universite Scientifique et Medicale de Grenoble. 277 p.

Maniar, P.D., Piccolli, P.M. 1989. Tectonic discrimination of granitoids. Geological Society of America Bulletin 101, 635-643.

Manning, C.E., Bohlen, S.R. 1991. The reaction titanite + kyanite = anorthite + rutile and titanite-rutile barometry in eclogites. Contributions to Mineralogy and Petrology 109, 1–9.

McDonough, W.F. 1991. Partial melting of subducted oceanic-crust and isolation of its residual eclogitic Lithology. Philosophical Transactions of the Royal Society of London Series a-Mathematical Physical and Engineering Sciences 335, 407–418.

Mirnejad, H., Lalonde, A. E., Obeid, M., Hassanzadeh, J. 2013. Geochemistry and petrogenesis of Mashhad granitoids: An insight into the geodynamic history of the Paleo-Tethys in northeast of Iran. Lithos 170–171, 105–116.

Moix, P., Beccaletto, L., Kozur, H.W., Hochard, C., Rosselet, F., Stampfli, G.M. 2008. A new classification of the Turkish terrenes and sutures and its implication for the paleotectonic history of the region. Tectonophysics 451, 7-39.

Muttoni, G., Mattel, M., Balini, M., Zanchi, A., Gaetani, M., Berra, F. 2009. The drift history of Iran from the Ordovician to the Triassic. The Geological Society, London, Special Publications 312, 7-29.

Omrani, H., Moazzen, M., Oberhansli, R., Tsujimori, T., Bosuqet, R., Moayyed, M.2013. Metamorphic history of glaucophane - paragonite-zoisite eclogites from the Shanderman area, northern Iran. Journal of Metamorphic Geology 31, 791-812.

Pearce, J.A. 1996. Sources and settings of granitic rocks. Episodes 19, 120–125.

Peccerillo, A., Barberio, M.R., Yirgu, G., Ayalew, D., Barbieri, M., Wu, T.W. 2003. Relationships between mafic and peralkaline silicic magmatism in continental rift settings: a petrological, geochemical and isotopic study of the Gedesma Volcano, Central Ethiopian Rift. Journal of Petrology 44 (11), 2003–2032.

Rezaeian, M., Carter, A., Hovius, N., Allen, M. B. 2012. Cenozoic exhumation history of the Alborz Mountains, Iran: New constraints from low-temperature chronometry. Tectonics, 31(2).

Ritz, J.F., Nazari H., Ghassemi, A., Salavati R., Shafei A., Solaymani S., Vernant, P. 2006. Active transtension

inside central Alborz: A new insight into northern Iran–southern Caspian geodynamics. Geology 34/ 6, 477–480.

Ruban, D.A., AL-Husseini, M.I., Iwasaki, Y. 2007. Review of Middle East Paleozoic plate tectonics. GeoArabia 12(3), 35-56.

Rudnick, R.L., Barth, M., Horn, I., McDonough, W.F. 2000. Rutile-bearing refractory eclogites: Missing link between continents and depleted mantle. Science, 287, 278–281.

Şengör, A.M.C. 1979. Mid-Mesozoic closure of Permo-Triassic Tethys and its implications. Nature 279, 590-593.

Şengör, A.M.C. 1990. A new model for the late Palaeozoic–Mesozoic tectonic evolution of Iran and implications for Oman. In: Robertson, A. H., Searle, M. P. & Ries, A. C. (eds) The Geology and Tectonics of the Oman Region. Geological Society, London, Special Publications 49, 797–831.

Shafaii Moghadam, H., Li, X.-H. Ling, X.-X. Stern, R. J., Khedr, M. Z. Massimo Chiaradia, M., Ghasem Ghorbani, G., Arai, S., Tamura. A. 2015. Devonian to Permian evolution of the Paleo-Tethys Ocean: New evidence from U–Pb zircon dating and Sr–Nd–Pb isotopes of the Darrehanjir–Mashhad "ophiolites", NE Iran. Gondwana Research 28, 781–799

Shellnut, J. G., Zhou, M.F., Zellmer, G.F. 2009. The role of Fe-Ti oxide crystallization in the formation of A-type granitoids with implications for the Daly gap: an example from the Permian Baima igneous complex, SW China. Chemical Geology 259, 204-217.

Shkodzinskiy, V.S. 1985. Magma Phase Evolution and Petrogenesis. Moscow: Nauka, 232 pp. [In Russian].

Stampfli G., Marcoux J., B., Baud, A.1993. Tethyan margins in space and time: In: Channell, J.E.T., Winterer, E. L., Jansa, L.F. (Eds). Palaeogeography, Palaeoclimatology and Palaeoecology 87, 373-409.

Stampfli, G.M., Kozur, H.W. 2006. Europe from the Variscan to the Alpine cycles. In: Gee, D.G., Stephenson, R.A. (Eds.), European lithosphere dynamics. Memoir of the Geological Society London, 57-82.

Stöcklin, J. 1974. Possible ancient continental margins in Iran. In The geology of continental margins (pp. 873-887). Springer Berlin Heidelberg.

Streckeisen, A. 1976. To each plutonic rocks its proper name. Earth Science Reviews 12, 1-33.

Sun, S.S., McDonough, W.F. 1989. Chemical and isotopic systematic of oceanic basalts; implications for mantle composition and processes. In: Saunders, A.D., Norry, M.J. (eds.) Magmatism in the ocean basins. Geological Society of London 42, 313-345.

Sylvester, P.J. 1989. Post-collisional alkaline granites. Journal of Geology 97, 261–280.

Taylor, R.P., Strong, D.F., Fryer, B.J. 1981. Volatile control of contrasting trace element distributions in peralkaline granitic and volcanic rocks. Contributions to Mineralogy and Petrology 77, 267–271.

Watson, E.B., Harrison T.M. 1984. Accessory minerals and the geochemical evolution of crustal magmatic systems: a summary and prospectus of experimental approaches. Physics of Earth and Planetary Interiors 35, 19–30.

Whalen, J.B., Currie, K.L., Chappell, B.W. 1987. A-type granites: geochemical characteristics, discrimination and petrogenesis. Contributions to Mineralogy and Petrology 95, 407-419

Zhanchetta, S., Zanchi, A., Villa, I., Poli, S., Muttoni, G. 2009. The Shanderman eclogites: a late carboniferous high-pressure event in the NW Talesh Mountions (NW Iran). Geological Society London, Special publications, 57-78.

Zanchi, A., Zanchetta, S., Berra, F., Mattei, M., Garzanti, E., Molyneux, S., Nawab, A., Sabouri, J. 2009. The Eo-Cimmerian (Late-Triassic) orogeny in North Iran. In: Brunet, M.-F.,Wilmsen, M., Granath, J. W. (eds) South Caspian to Central Iran Basins. Geological Society of London Special Publications 312, 31–55.

Zhang, C.-Z., Li B., Cai, J.-X.a, Tang X.-C., Wei, Q.-G., Zhang, Y.-X. 2008. A-type granite and adakitic magmatism association in Songpan-Garze fold belt, eastern Tibetan Plateau: Implication for lithospheric delamination: Comment. Lithos 103, 562–564.